Astron. Astrophys. 319, 637–647 (1997)

ASTRONOMY
AND
ASTROPHYSICS

The spectrum of β Coronae Borealis in the lithium region

M. Hack[1], **N.S. Polosukhina**[2], **V.P. Malanushenko**[2], **and F. Castelli**[3]

[1] Dipartimento di Astronomia, via G.B.Tiepolo 11, I-34131 Trieste, Italy
[2] Crimean Astrophysical Observatory, p/o Nauchny, 334413 Crimea, Ukraine
[3] CNR-Gruppo Nazionale Astronomia and Osservatorio Astronomico, via G.B. Tiepolo 11, I-34131 Trieste, Italy

Received 22 March 1996 / Accepted 5 August 1996

Abstract. Results from spectroscopic observations in the Li region of the binary CP star β CrB (HD 137909, HR 5747, F0p) are presented. The observations were carried out at the Crimean Observatory from 1993 to 1995 with the coudé spectrograph equipped with a CCD detector, R=45000.

We have analyzed the 6693-6721 Å region by means of the spectral synthesis method by assuming a model with parameters $T_{\rm eff}$=8000 °K, $\log g$ = 4.0, and $[M/H]$ = 1.0. We derived abundances for the elements with lines in the studied range. The observed feature at 6708 Å is not well fitted by the Li doublet even by assuming an isotopic ratio 10 times the terrestrial value and an overabundance of lithium of 2.6 dex; a very good fit is obtained assuming a blend with V I at 6708.094 Å, in the hypothesis that Vanadium is in excess by a factor larger than 10^3 (a value which is not confirmed by other abundance determinations). It is more probable that the Li feature is blended with some unidentified line due to some overabundant heavy element.

The ultraviolet excess for $\lambda < 1600$ Å is discussed. It could be explained either by assuming that the companion is a λ Boo star having a metal deficiency $[M/H] = -1.0$ and $T_{\rm eff} \sim 8200° K$, or by assuming that β CrB is Si deficient, so that the Si I discontinuities at 1514.34 Å and at 1674.03 Å disappear. However, there is no clear evidence of underabundances of this element with respect to the solar value.

The main results of this paper are: the variability of the lithium blend with the period of rotation of the star; the relations between rotational radial velocity, line intensity W_λ and FWHM variations for the Li blend and other lines of different elements - Fe , Gd , Ce - which show similar variations.

Key words: stars: abundances – stars: chemically peculiar – lines: identification – individual star: β CrB

1. Introduction

During many years, starting with 1963 (Faraggiana & Hack, 1963), some investigators on CP stars started to pay attention to the problem of lithium. The identification of Li doublet was doubtful because of the relatively low spectral resolution and S/N ratio. Moreover the problem is complicated by some effects typical of CP stars, like the presence of strong magnetic fields, inhomogeneity in chemical composition at the surface, and different Doppler shifts of lines of different ions with the rotation of the star, and even with rapid, non-radial oscillations on time scales of minutes (Kurtz et al., 1994a, 1994b, 1994c). The technique of Doppler imaging has been applied to several of these stars in order to map the repartition of some elements on their surface; it has been shown that the abundance anomalies are distributed in spots or rings, whose location is related with the magnetic field structure (Hatzes, 1991a, 1991b).

The more recent observations of Li in CP stars, obtained with modern equipments indicate that Li doublet is possibly present in the spectra of some CP stars. However, the presence of several lines of Gd and Ce and of some unidentified features in the same spectral region suggests the possibility that the main component of the Li blend may be due to some unidentified line, and the problem is still open.

The observations of Ap stars in the Li region with modern detectors were carried out by Faraggiana et al. (1986) and concerned a dozen of Ap stars of different types and effective temperatures, including a few stars with $T_{\rm eff} \geq 10000$ ° K, where Li would be unobservable, unless it is enormously overabundant. This survey, supplemented by Gerbaldi & Faraggiana (1991), showed that some Ap stars are Li poor, while others may be strongly Li rich. However, only few observations per star were made, and so the behavior of the Li feature versus the rotational phase was not examined. This type of observations began at the Crimean Observatory for some Ap stars and suggested that this element may be overabundant in β CrB and γ Equ (Polosukhina & Lyubimkov,1995). A shift of λ 6708 Å correlated with the phase of rotation was observed in β CrB and the hypothesis of a different distribution of the Li abundance over the surface of the star may be advanced.

We analyzed the 6693-6721 Å region of β CrB in order 1) to obtain a correct identification of the lines, and 2) to derive abundances. We have used the synthetic spectrum method. Atmospheric models were computed with the ATLAS9 code (Kurucz, 1993a) and synthetic spectra were computed with the

Send offprint requests to: M. Hack

Table 1. The observations

(1)	(2)	(3)	(4)	(5)	(6)	(7)
		JD 2449000+	S/N	Mean phases	Orbital phases	N
93-06-06	6708	145.392	370	0.4805	0.1939	1
93-06-15	6708	154.365	180	0.9659	0.1962	1
93-06-21	6708	160.347	380	0.2895	0.1977	1
93-06-22	6708	161.335	510	0.3429	0.1980	1
93-06-23	6708	162.341	280	0.3973	0.1982	1
94-02-24	6707	408.469	350	0.7113	0.2618	2
94-02-25	6707	409.486	200	0.7665	0.2621	2
94-03-25	6707	437.490	670	0.2814	0.2693	2
94-07-04	6707	538.379	500	0.7384	0.2953	2
94-07-05	6707	539.380	560	0.7925	0.2956	2
94-09-09	6707	605.326	290	0.3593	0.3126	1
94-09-10	6707	606.305	430	0.4123	0.3129	1
95-03-05	6707	782.533	460	0.9453	0.3584	2
95-06-26	6707	895.287	470	0.0444	0.3875	2
mean			1590	0.54	0.267	21

(1) Date
(2) Region
(3) HJD
(4) S/N ratio
(5) Phase of rotation ($pos.cross$ = $2434217^d.50 + 18^d.487\times$ E)
(6) Phase of orbital motion (by Oetken & Orwert (1984): $2425156^d.541 + 3873^d.0\times$ E)
(7) Number of spectra

SYNTHE code (Kurucz, 1993b). Line lists are mostly based on the Kurucz data (Kurucz,1993b).

2. Observations and spectra reduction

The observations of β CrB were carried out in 1993-1995 with the coudé spectrograph of the 2.6 meter telescope of the Crimean Astrophysical Observatory, equipped with a CCD camera with red- sensitive GEC detector, 600×400 pixel array. The spectral resolution is 45000. The typical S/N ratio is better than 200. The mean exposure time is about 20 - 30 minutes. Table 1 lists the observations of β CrB.

The reduction of the spectra was made using the software SPE written by S. Sergeev at the Crimean Observatory. A detailed description of these operations is given in Sergeev (1996).

For the lithium problem it is very important to determinate the wavelength scale with great accuracy. The majority of the observers of this spectral region make differential measurements of the position of the Li blend by using either some Fe I lines (Polosukhina & Lyubimkov, 1995) or the line of Ca I at λ 6717.685 Å (Smith et al., 1993) as reference lines. For metal-poor stars the method of differential measurements is correct, because the probability of blending is very low, and the accuracy obtained for the position of the Li line is high (about 0.003 Å). But in the case of β CrB the spectrum is very rich of metallic lines and there are no Fe I lines free from blends. The accuracy of the determination of the Li line position becomes worse than 0.02 Å. Therefore, in order to obtain a larger precision for the wavelength scale, we used for the present analysis two comparison spectra of thorium (one above and one below the stellar spectrum). We used typically 8 to 12 comparison lines. The typical error for the position is equal to FWHM/(S/N). In our case, a line of the comparison spectrum has FWHM = 0.15 Å , S/N from 20 to 120, hence σ from 0.0075 Å to 0.0012 Å. The standard deviation of the dispersion curve from the polynomial fitting is 0.002 - 0.003 Å . Since we study a short spectral region, 31 Å, we used a first degree polynomial for fitting the dispersion curve. Hence we derived the wavelength scale from the comparison spectra for each stellar spectrum. After normalization of each spectrum to the continuum, we made the following operations:

1) All spectra of β CrB were shifted to the position of the spectrum corresponding to phase $0^p.046$ of the rotational period. This phase is near to the phase of crossover, and we use it as reference. The value of the shift was derived by cross-correlation function between each spectrum and that at phase $0^p.046$.

2) We determined a mean spectrum from all the observations. We used the laboratory wavelength of Ca I 6717.685 Å as reference in the mean spectrum. The result of the first iteration was the value of the shift of the center of gravity of this Ca I line in the mean stellar spectrum to the position in the laboratory wavelength scale. Then each individual spectrum was shifted to the laboratory wavelength scale. The result of the next iteration using cross-correlation function for the individual spectra is the mean spectrum of β CrB, with S/N = 1590 in the laboratory wavelength scale. The individual spectra are shown in Fig. 1.

The shifts of the individual spectra needed to obtain the mean spectrum were used for deriving the position and possible variations with the stellar rotation of the center of gravity of the Li feature and of some other lines.

The mean spectrum is used for comparison with the synthetic spectrum and for the determination of the abundance of Li and other elements showing lines in this spectral region (Sect. 3).

3. The spectral analysis with the synthetic spectrum method

One of the most accurate methods to derive stellar abundances is based on the comparison of the observed spectrum with a synthetic spectrum. This approach requires the selection of an atmospheric model for the studied star. The main parameters of the model are the effective temperature $T_{\rm eff}$, the surface gravity $\log g$, the metallicity $[M/H]$, and the microturbulent velocity ξ.

We assumed as first estimate $[M/H]$ = 1.0 according to previous determinations for the iron abundance (Adelman, 1973; Savanov & Malanushenko, 1990) and $\log g$ = 4.0 from Faraggiana & Gerbaldi (1992). We assumed an "a priori" microturbulent velocity equal to 2 km s^{-1}. Then, we derived the effective temperature from the comparison of observed and computed energy distributions. Observed energy distributions are the visual spectrophotometric observations from Pyper & Adelman

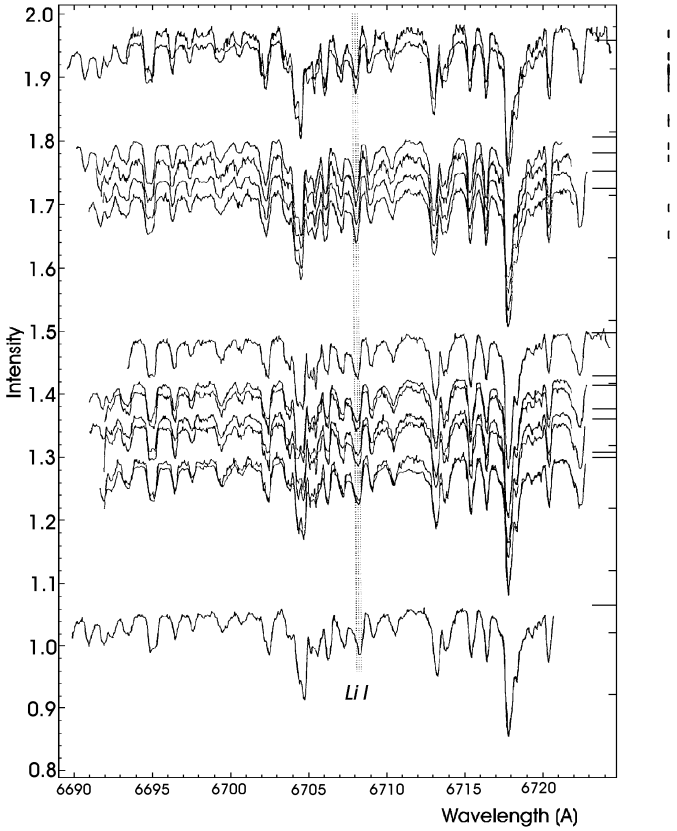

Fig. 1. The individual spectra of β CrB at different rotational phases. From top to bottom: rotational phases 0.96, 0.94, 0.79, 0.77, 0.73, 0.71, 0.48, 0.41, 0.40, 0.36, 0.34, 0.29, 0.28, 0.04.

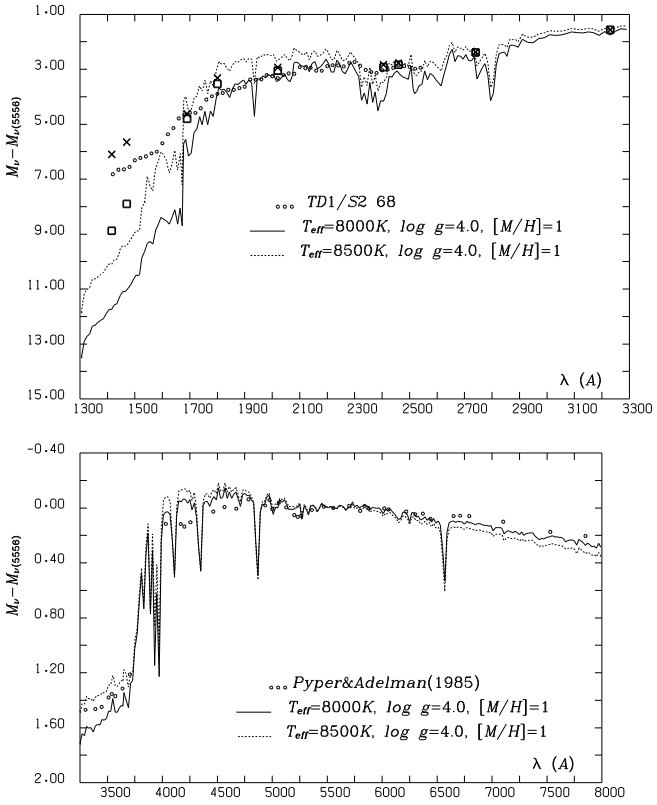

Fig. 2. Observed and computed energy distributions. The crosses indicate the energy distribution obtained by assuming the presence of a λ Boo companion with $T_{\rm eff}$= 8500 °K and the squares indicate a λ Boo companion with $T_{\rm eff}$= 8000 °K.

(1985) and from the Breger (1976) catalog and the UV data from the TD1 S2/68 experiment (Jamar et al., 1976). Computed energy distributions were derived from Kurucz (1993a) models.

Fig. 2 shows the comparison of the observed energy distributions with those corresponding to models having effective temperatures equal to 8000 °K and 8500 °K respectively. The best agreement between the observed and computed visual and ultraviolet ($\lambda > 1650$ Å) fluxes is yielded by the model with $T_{\rm eff}$= 8000 °K. The disagreement shortward λ 1650 Å, where the Si I discontinuities at 1514.35 Å and 1674.03 Å occur, may partly be due to a Si abundance lower than 10 times the solar one, as it was assumed for the model. However, previous determinations (Adelman 1973, Savanov & Malanushenko, 1990) indicated solar abundance for Si. In this paper we found solar abundance as upper limit, because no Si lines were observed in the $\lambda\lambda$ 6693-6721 Å range. On the other hand, comparison with few stars observed with TD1 S2/68 of about the same spectral type or earlier, indicates an ultraviolet excess of β CrB (Table 2).

β CrB is the primary member of a spectroscopic binary system with a companion which has about the same spectral type, since from visual observations m_B - m_A is about constant and equal to 1.6^m (Kamper et al., 1990). No spectral lines of the companion have never been detected. Now, if we assume that the companion is a λ Boo star with high rotational velocity and $[M/H] = -1.0$ the UV excess could be explained. Table 3 gives the energy distribution obtained by summing up the flux F_A and F_B. F_B is obtained from the model for $[M/H] = -1.0$ divided by 5 and F_A from the model for $[M/H]$ = 1.0 multiplied by 4/5, F_A/F_B = 4 corresponding to m_B - m_A = 1.5^m. Assuming for β CrB$_B$ $T_{\rm eff}$= 8000 °K, the UV excess is still lower than the observed one, while assuming $T_{\rm eff}$ = 8500 °K the UV excess is slightly larger than the observed one. A λ Boo companion with

Table 2. Ultraviolet magnitude differences for β CrB compared with other stars of similar spectral type (data derived from fluxes observed with TD1-S2/68)

	β CrB F0p	α Aql A7 IV - V	ι UMa A7 V	γ Her A9 III	HD55892 F0 V	α Pic A5 V
$m_{1420} - m_{2740}$	+2.96	+5.47				
$m_{1540} - m_{2740}$	+2.49	+3.77				+2.89
$m_{1600} - m_{2740}$	+2.09	+2.52	+3.40			+1.93
$m_{1680} - m_{2740}$	+1.15	+1.25	+1.52	+2.13	+2.02	+1.01

Table 3. Observed energy distribution and that computed assuming the presence of a λ Boo companion

Wavelength (Å)	Theoretical model (1)	Theoretical model (2)	Theoretical model (3)	Observed energy distribution $m_\lambda - m_{\lambda 5500Å}$
5500	+0.00	+0.00	+0.00	+0.00
4225	+0.00	+0.00	−0.03	+0.00
3600	+1.40	+1.40	+1.36	+1.42
3230	+1.60	+1.56	+1.56	+1.60
2740	+2.60	+2.39	+2.38	+2.50
2460	+3.10	+2.83	+2.78	+2.80
2405	+3.10	+2.92	+2.83	+3.00
2020	+3.20	+3.05	+2.93	+3.21
1800	+3.80	+3.53	+3.31	+3.81
1690	+5.80	+4.80	+4.62	+4.80
1470	+11.00	+7.90	+5.65	+6.80
1415	+11.80	+8.88	+6.10	+6.92
$m_{1415} - m_{2740}$	+9.20	+6.49	+3.72	+4.42

Notes:
1) Kurucz theoretical model for $T_{\rm eff}$= 8000 °K, log g = 4.0, $[M/H]$ = 1.0
2) Kurucz theoretical models. The total flux $F = 0.8 \times F_A + 0.2 \times F_B$, where F_A is the model for $T_{\rm eff}$= 8000 °K, log g = 4.0, $[M/H]$ = 1.0 and F_B is the model for $T_{\rm eff}$= 8000 °K, log g = 4.0, $[M/H] = -1.0$
3) Same as 2), but F_B is the model for $T_{\rm eff}$= 8500 °K, log g = 4.0, $[M/H] = -1.0$.

parameters $T_{\rm eff} \sim$ 8200 °K, log g = 4 and $[M/H] = -1.0$ can explain the observed UV excess (Table 3).

The Balmer discontinuity is the only feature in the energy distribution dependent on gravity. For $T_{\rm eff}$=8000 °K, it is reproduced at best by the model with log g = 4.0.

To analyse the high resolution spectrum in the range $\lambda\lambda$ 6693 - 6721 Å we computed synthetic spectra with the SYNTHE code (Kurucz, 1993b) and compared them with the mean spectrum. As input data we used the ATLAS9 model with parameters $T_{\rm eff}$= 8000 °K, log g = 4.0, $[M/H]$ = 1.0, ξ = 2 km s^{-1}, and the Kurucz (1993 b) line lists, with some modifications. For all the Fe I lines of the Li region we adopted wavelengths, energy levels, and log gf from Nave et al. (1994), when available. For Fe I 6712.676 Å , log $gf = -2.877$ from Kurucz (1993b) was replaced by log $gf = -3.63$, on the basis of the agreement between the observed and computed features both in β CrB and Procyon. In fact , we used the Procyon atlas from Griffin & Griffin (1979) to check the wavelength scale of β CrB and to estimate the reliability of the atomic data for the few lines common to the two stars. A model with parameters $T_{\rm eff}$= 6500 °K, log g = 4.0, and ξ=2 km s^{-1} was used for Procyon. For Li at 6708 Å we considered both the isotopes Li^6 and Li^7 and all the hyperfine structure components listed in Kurucz (1995).

As first iteration for the synthetic spectrum, we assumed abundances 10 times the solar ones for all the elements. The spectrum was broadened for a gaussian instrumental profile corresponding to a resolving power of 45000. To match the observed and computed wavelength scale, the observed spectrum was shifted toward the red by 3 km s^{-1}, corresponding to a wavelength shift $\Delta\lambda$=0.07 Å . Then, as a second step, we decreased the abundances of C, Al, and Si, owing to the predicted presence of some lines which were not observed, and, at the same time, we increased the abundances of Li, La, Ce, Sm, and Gd owing to the presence in the spectrum of observed lines much stronger than the predicted ones.

After several trials with different values for the rotational velocity v*sin i*, we estimated that v*sin i* = 11 km s^{-1} is the best suited value to reproduce the observed spectrum. Actually the rotational velocity, derived by the stellar radius and the rotational period of 18.5 days is about 3.5 km s^{-1}, hence the broadening is mainly due to the magnetic field. Our choice agrees with the value v*sin i*$\leq$ 11.2 km s^{-1} found by Mathys (1995).

The range $\lambda\lambda$ 6693 - 6721 Å is too short and there are too few lines in it in order to determine a value for the microturbulent velocity ξ. The comparison of synthetic spectra computed with different values of ξ (0, 2, and 4 km s^{-1}) has shown that the only lines affected by ξ in an appreciable way are Gd II at 6694.867 Å and 6702.093 Å , the blend Gd II and Ce II at 6704.147 Å and 6704.524 Å , Ce II at 6706.051 Å , the blend Ca I and Gd II at 6717.681 Å and 6718.130 Å , and finally Ce II at λ 6720.280 Å . Because there are no other lines of Gd , Ce and Ca weak enough to be independent from ξ we have been not able to estimate any value for the microturbulent velocity and we arbitrarily assumed it equal to 2 km s^{-1}. Therefore, the abundances derived for Gd , Ce and Ca depend on this choice of ξ.

After having fixed the wavelength scale, the rotational velocity, and the microturbulent velocity, we modified the abundances until we obtained the best agreement between the observed and computed spectra. The final abundances are listed in the last column of Table 4. Abundances from previous determinations are also given for comparison. In Fig. 3 the mean observed spectrum is compared with the final computed spectrum. The Li blend was computed with the terrestial ratio Li^6/Li^7=0.081 (Anders & Grevesse, 1989). The upper plot shows the computed spectrum not broadened for rotational velocity and magnetic field, the lower plot shows the computed spectrum broadened for v*sin i*=11 km s^{-1}.

The upper plot of Fig. 3 shows that, owing to the lack of atomic data, several features are still unidentified, so that it is very hard to obtain a good agreement between the observed and the computed spectra. The lower plot shows that the agreement is not very good also when the lines are well identified. In fact for β CrB, in addition to the usual problems occurring when observed and computed spectra are compared (difficulty in placing the continuum, uncertainty in the log gf values and line wavelengths, lack of atomic data), there are also problems due both to the spectrum variability, and to the effect of the magnetic field which was not considered in our computations. For instance, the comparison of two spectra taken at two different phases shows that several lines have different intensities, in particular the lines of Ce II and Gd II (see Fig. 1). The conclusion is that the final

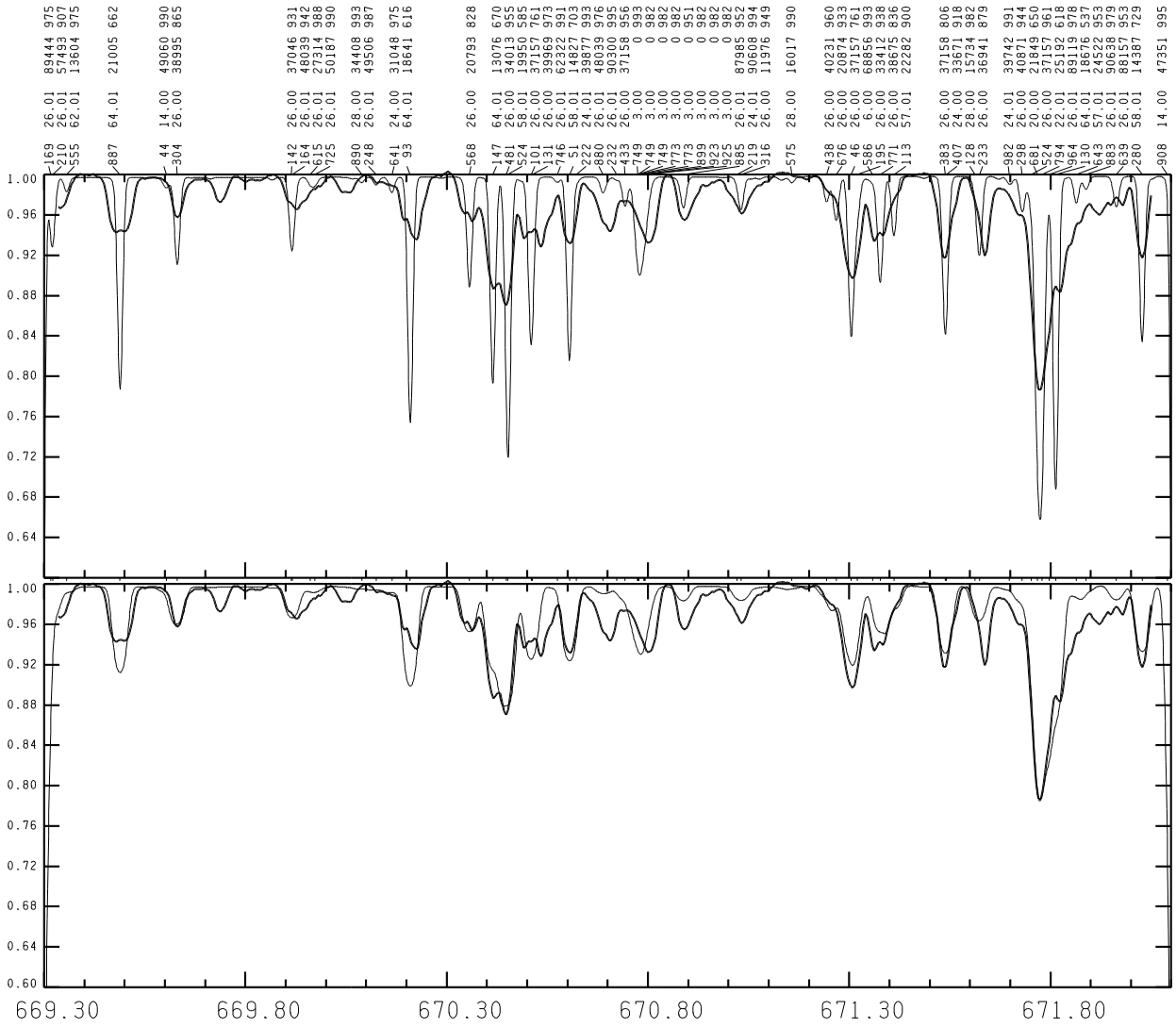

Fig. 3. Comparison of the observed spectrum (thick line) in the Li region with the synthetic spectrum (thin line) computed for a model with $T_{\rm eff}$=8000 K, log g = 4.0, $[M/H]$ = 1.0, abundances listed in last column of table 4, and microturbulent velocity ξ=2 km s^{-1}. Upper plot: the computed spectrum is not broadened for the rotational velocity. Lower plot: the computed spectrum is broadened for a rotational velocity v *sin i*= 11 km s^{-1}.

abundances of Table 4 have to be considered only estimates to be used as starting point for further analyses which will take into account also the magnetic field effects.

Landstreet (1996) discusses the several effects of magnetic field and surface inhomogeneities which lead to systematic errors when spectra are modeled using conventional spectrum synthesis codes. He concludes that the standard method treating "the abundances as constant over the visible disk should be able of getting reasonably useful abundances (accurate within a factor of two or three compared to the real abundances averaged over the central part of the visible hemisphere)". Hence, in the case of β CrB, the abundances derived from a spectrum averaged over the whole rotational period should be accurate enough to show the abundance pattern of this magnetic peculiar star. A confirmation of this remark is given by the reasonably good agreement among determinations of abundances obtained at different epochs and in different spectral regions by different authors (Table 4).

4. The lithium doublet

The Li I doublet is formed by two Li^7 components at 6707.761 Å and 6707.912 Å . The very fragile Li^6 isotope can also be observed in some stars. Its components lie at 6707.921 Å and 6708.072 Å . If the hyperfine structure is also considered the number of the Li^7 + Li^6 components may amount up to 19 lines (Kurucz, 1995).

The terrestrial "representative isotopic ratio" is tabulated to be equal to 0.081 by Anders & Grevesse (1989), while the meteoritic value representative of the early solar system is 0.079 (Anders & Ebihara, 1982). We assumed the isotopic ratio from

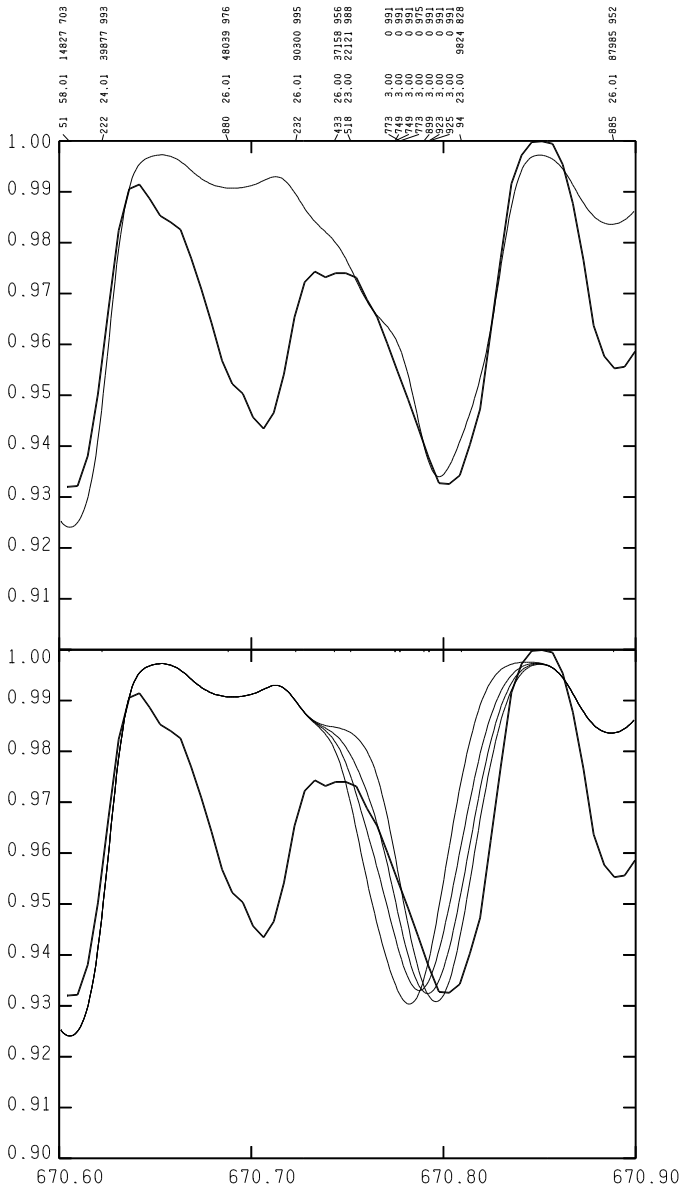

Fig. 4. Upper plot: The observed Li feature (thick line) compared with that computed for an isotopic ratio 0.081, $\log(N_{Li}/N_H) = -8.54$, and $\log(N_V/N_H) = -4.80$. Lower plot: The observed Li feature (thick line) and the computed ones for $\log(N_{Li}/N_H) = -8.24$ and different isotopic ratios. From left to right: Li^6/Li^7 = 0.081, 0.7, 2, 10.

Anders & Grevesse (1989) as starting point for our computations. However, in the case of peculiar stars, especially for cold CP stars, the strong surface magnetic fields can make the Li problem very complicate, because they hamper the mixing of surface matter with the internal hotter one.

The lower plot of Fig. 4 shows that in the case of β CrB the feature at 6708 Å can not be reproduced by computations with a Li abundance $\log(N_{Li}/N_H) = -8.24$ (i.e. 2.6 dex larger than the solar one) and an eventual Li^6/Li^7 ratio equal to 0.081. In fact, the observed feature is redshifted by 0.2 Åwith respect to the computed one. When the isotopic ratio is increased, the wavelength difference between the observed and computed absorptions slightly decreases, but it is never eliminated even if a highly improbable isotopic ratio equal 10 is assumed. All the 19 isotopic and hyperfine components listed in Kurucz (1995) were considered in the computations.

Table 4. The abundances $[M/H]$ of β CrB relative to the solar ones from Anders & Grevesse (1989) are compared with previous determinations.

Element	H(58)	A(73)	SM(90)	SM(90) *	Present **
Li					+2.60:
C					$\leq$-0.90
N					$\leq$ 0.00
Mg	+0.2	0.0			
Al					$\leq$-1.20
Si		+0.2	+0.11	+0.06	$\leq$ 0.00
Ca	+0.1	+1.6	+0.38	+0.57	+0.30
Sc	+0.4	+2.0	+0.80	+0.63	
Ti	+0.9	+1.5	+1.03	+1.04	
V	+0.4	+0.8	+0.52	+0.51	+1.00
Cr	+1.5	+1.8	+2.18	+2.0	+1.70
Mn	+1.6	+1.7	+1.5	+1.5	
Fe	+0.8	+1.3	+1.0	+0.85	+1.10
Co	+1.0	+1.6	+1.48	+1.47	
Ni	+0.3	+0.8	+1:	+1:	+1.00
Sr	+1.6	+1.9	+2.42	+2.35	
Y		+0.7	+0.73	+0.79	
Zr	+2.0	+2.3	+1.96	+1.81	
Ba	+0.7	+0.6	+0.89	+1.28	
La	+2.8				+2.65
Ce	+2.9	+2.7	+2.12	+1.94	+3.40
Sm	+2.3	+3.6	+1.96	+1.85	+2.00
Gd	+2.9	+3.7	+2.79	+2.58	+3.90
U			+2.83	+2.58	

Notes: H(58) = Hack, 1958; A(73) = Adelman, 1973; SM(90) = Savanov & Malanushenko, 1990 ; SM(90) * abundances corrected fo the presence of the secondary; present work **

Another explanation of the observed redshifted feature with respect to the Li I predicted wavelength is the blending of Li I with some other element. From the analysis of the known atomic lines in the 6707.0 - 6708.6 Å region listed in Table 7 of Gerbaldi et al. (1995) and used by us for computing the spectrum of β CrB, we could infer that V I at 6708.094 Å is the only possible component to the 6708 Å feature observed in β CrB. Because it is not predicted in the Sun (Gerbaldi et al., 1995; Kurucz, 1995) we modified the $\log gf = -3.113$ from Kurucz (1993b) until we obtained a predicted feature consistent with the solar observations. In this way we fixed $\log gf = -1.813$ for V I 6708.094 Å . Then we modified the Li and V abundance of β CrB in order to fit the feature at 6708 Å with the computations. The upper plot of Fig. 4 shows the comparison of the observed spectrum with a spectrum computed with $\log(N_{Li}/N_H) = -8.54$ and $\log(N_V/N_H) = -4.80$ (i.e. 3.2 dex larger than the solar value). The agreement is good and further-

Table 5. List of all the lines contributing to the spectrum of β CrB in the lithium region

Elem.	λ	Elem.	λ	Elem.	λ
Fe II	6693.169	Fe II	6705.746	Fe I	6713.771
Fe II	6693.210	Ce II	6706.051	La II	6714.113
Sm II	6693.555	N I I	6706.107	Fe I	6715.383
Gd II	6694.887	Cr II	6706.222	Cr I	6715.407
Si I	6696.044	Fe II	6706.880	Ni I	6716.128
Fe I	6696.304	Fe II	6707.232	Fe I	6716.233
Fe I	6699.142	Fe I	6707.433	Cr II	6716.982
Fe II	6699.164	Li I	6707.749	Fe I	6717.298
Fe II	6699.615	Li I	6707.773	Fe I	6717.524
Fe II	6699.725	Li I	6707.899	Ca I	6717.681
Ni I	6699.890	Li I	6707.923	Ti II	6717.794
Fe II	6701.248	Li I	6707.925	Fe II	6717.964
Cr I	6701.641	Fe II	6708.885	Gd II	6718.130
Gd II	6702.093	Cr II	6710.219	La II	6718.643
N I	6702.862	Fe I	6710.316	Fe II	6718.883
Fe I	6703.568	Ni I	6710.575	Fe II	6719.639
Gd II	6704.147	C I	6711.323	Ce II	6720.280
Fe I	6704.481	Fe I	6712.438	Si I	6720.908
Ce II	6704.524	Fe I	6712.676		
N I	6704.839	Fe I	6713.046		
Fe I	6705.101	Fe I	6713.195		
Fe I	6705.131	C I	6713.586		

more the large vanadium abundance does not yield in the $\lambda\lambda$ 6693 - 6721 Å region strong vanadium lines predicted but not observed. Anyway, other wavelength ranges should be studied in order to check this high V abundance. In fact, previous works (see Table 4) have given V in excess by a factor lower than 10.

The last, most acceptable hypothesis, is that lithium is blended with some unknown element, possibly belonging to the heavy elements or to rare earth elements, which were found overabundant by factors ranging from 10 to 1000 (see for instance the abundances of Sr, Zr, La, Sm, Gd, Ce listed in Table 4). Actually some unidentified features are present in the studied region. The strongest ones are at 6697.3, 6700.4, 6705.0, 6707.0, 6709, 6710.3, 6713.6, 6716.3 Å (Fig. 3). For instance, from a comparison of giants with different gravities, Lambert et al. (1993) concluded that in stars enriched in heavy elements, a Ce II line could blend the Li line. Since, in β CrB, Ce II is overabundant by $2 \div 3$ dex, a similar blending can be expected.

Finally, we have not investigated the effect of the magnetic field on the Li line. In fact, accurate determinations of the abundances in magnetic stars require to take into account the broadening by the magnetic field.

We have searched for the presence of the other Li I line at 6103.64 Å in spectra of β CrB observed by us in this region. This Li I line is not observable, as expected, because it is fainter than the resonance doublet and is blended with a strong Fe II line at 6103.54 Å .

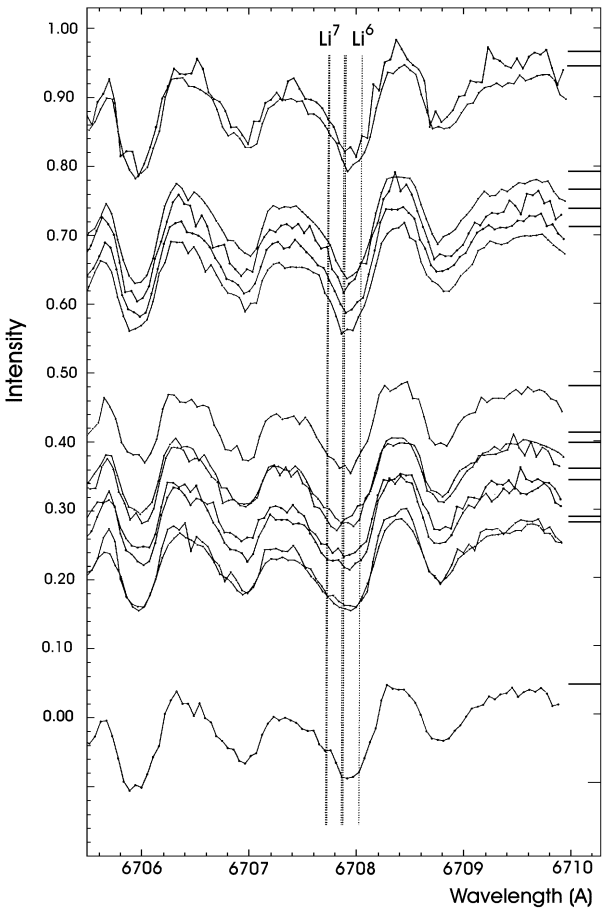

Fig. 5. The variation of the Li feature with the rotational phase. From top to bottom: rotational phases 0.96, 0.94, 0.79, 0.77, 0.73, 0.71, 0.48, 0.41, 0.40, 0.36, 0.34, 0.29, 0.28, 0.04.

5. Variability of the line parameters: V_r, W_λ, FWHM

The feature at 6708 Å is present in all the spectra. As we discussed in the previous sections, the contribution to the blend is probably due to the Li I resonance doublet, to the V I line and to some other unknown element.

The behavior of the profiles of the 6708 Å blend versus the rotational phase is shown in Fig. 5. It can be seen that the line is an asymmetric blend with a well defined red wing and a more shallow blue wing. The profile of the blend undergoes evident changes during the rotational period. The most simple way to interpret these variations is to suppose that the feature consists of two components, red and blue with somewhat variable intensity and wavelength. The strength of the blue component probably changes in antiphase with the red component. Rotational Doppler effect is visible in the line profiles.

Fig. 6 shows the variations of position of the center of gravity of some lines in the Li region, expressed by the rotational radial velocity V_r (km s^{-1}) versus the rotational phase of β CrB. We believe that the variation of the line position is a real effect, but the number of the available observations for the phases $0^p.00$ - $0^p.20$, $0^p.50$ - $0^p.70$ is insufficient for the

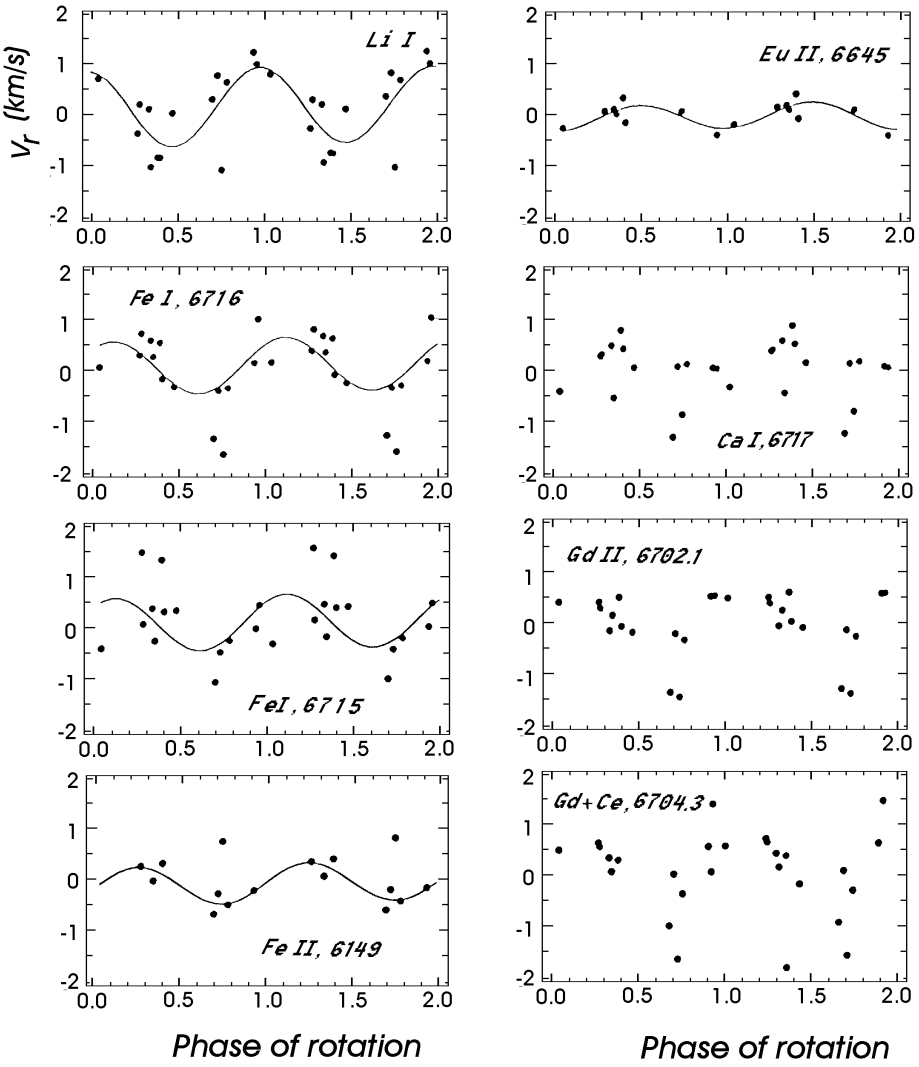

Fig. 6. Rotational radial velocity V_r versus the rotational phase.

determination of the accurate shape of the rotational radial velocity curve. The full amplitude of the V_r variations is consistent with the projected rotational velocity of β CrB (v *sin* $i \sim$ 2-3 km s^{-1}, Preston, 1967). The maximum amplitude of the V_r variations is shown by the lines 6702.10 Å Gd II, and 6704.3 Å Gd II+Ce II. Our observations indicate that most of the lines vary with the period of rotation. For completeness of presentation of the spectral variability, we have used also other spectral regions: λ 6645 Å Eu II, and λ 6149 Å Fe II. The behavior of these lines is similar to those of the Li region, but with different amplitudes. The typical scattering from the curve of rotational radial velocity for the Li region is about 0.3 - 0.5 km s^{-1}.

Fig. 7 and 8 show the results of our measurements of the equivalent widths W_λ and full width at half maximum FWHM with the rotational phase. The behavior of each line is different. The maximum amplitude of the curve W_λ versus rotational phase is shown by the blends 6704 Å Gd II + Ce II and 6706 Å Fe I + Ce II, while the lines of Fe I at $\lambda\lambda$ 6149, 6702 , 6716, and 6715 Å almost do not vary, and λ 6702 Å Gd II shows small variations; therefore the more variable lines are probably those of Ce II. The equivalent width of the Li blend does not vary very much, while the FWHM shows remarkable variations. The FWHM of lines of Fe I and Eu I do not vary in an appreciably way.

The data giving the relations V_r, W_λ , and FWHM versus the rotational phase are sufficiently well defined only for few lines. The FWHM is almost constant for the lines examinated, with the exception of λ 6708 Å. The maximum and the minimum FWHM are observed at rotational phases $0^p.3$ and $0^p.8$ respectively. At phase $0^p.3$ the equivalent width has its maximum value while at phase $0^p.8$ has a medium value. When the rotational radial velocity V_r is at the maximum and minimum values (i.e. the lithium + other contributors are concentrated at the borders of the stellar disk) the FWHM is at its medium and not at the minimum value, as we should expect. Hence the relations between V_r, W_λ, and FWHM are not easily interpretable and possibly indicate the presence of several concentrations of different intensities.

The only two other lines for which we have reasonably well defined curves both for the equivalent width and the rotational radial velocity are λ 6702 Å Gd II and the blend 6704 Å Gd II

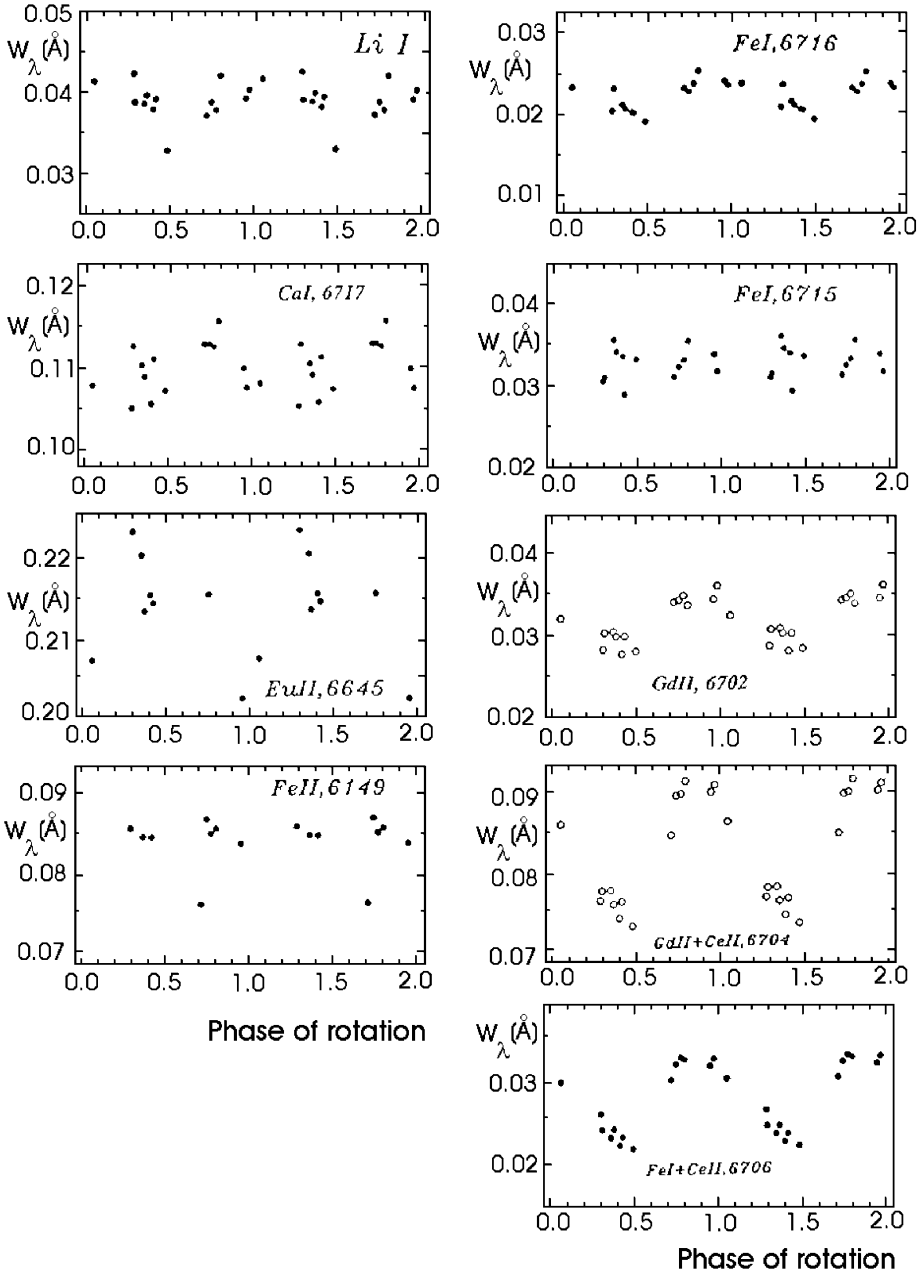

Fig. 7. The equivalent widths W_λ versus the rotational phase.

+ Ce II. They show roughly the same behavior, with W_λ at its medium value when the rotational radial velocity is at maximum and minimum values, and W_λ is maximum when V_r has its medium value; this behavior can be explained by one large spot where Gd and Ce are concentrated.

λ 6706 Å Fe II + Ce II shows a very well defined curve W_λ versus rotational phase, in phase with those for $\lambda\lambda$ 6702 and 6704 Å , but no rotational radial velocity curve was available.

λ 6716 Å Fe I shows two curves with smaller amplitude than those for $\lambda\lambda$ 6702, 6704, and 6706 Å and a different behavior, with W_λ at maximum for V_r varying from its medium to its maximum value and W_λ at medium value for medium value of V_r. The full analysis of the correlations between the variations of V_r, W_λ, and FWHM need more observations.

We interpret the asymmetric absorption feature λ 6708 Å (Fig. 5) as due to the blend of two components with variable center of gravity of each component. A possible explanation is a spotted distribution of lithium and other unknown blending elements on the stellar surface. A source of uncertainty both for the study of the variations of the rotational radial velocity versus the rotational phase and for fixing the position of the 6708 Å feature is not a sufficient precision in the wavelength scale. We have made corrections to the wavelength scale after a critical analysis of the binary radial velocity curve (Polosukina & Malanushenko, 1995) using the numerous measurements of radial velocity by Neubauer (1944), Oetken & Orwert (1984) and Kamper et al. (1990). The difference between the orbital elements by Oetken & Orwert and Kamper et al. cannot be ne-

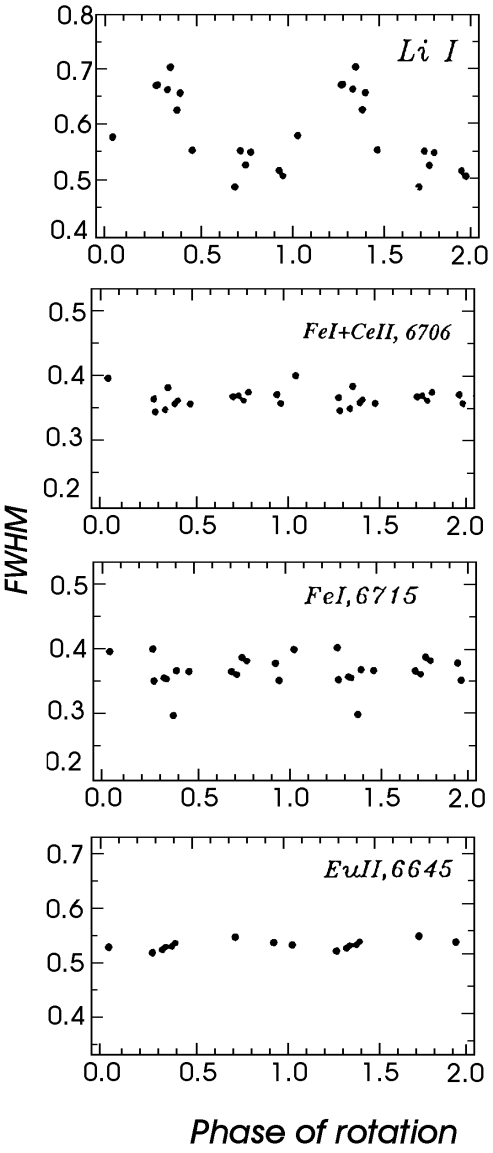

Fig. 8. FWHM versus the rotational phase.

glected, because the orbital radial velocity curve presents a very deep and narrow minimum, and the position of the minimum depends on the accuracy in the determination of the period. Since the value of the period is not defined with sufficient precision (only two decimal figures), it is impossible to obtain a very accurate determination of the position of the spectral lines, which is necessary in our study of the Li feature, especially for the observations made in 1990 - 92 which fall near the minimum of the orbital radial velocity curve.

6. Conclusion

The energy distribution longward 1650 Å is well fitted by the model with parameters $T_{\rm eff}$= 8000 °K, $\log g$ = 4.0, and solar scaled abundances $[M/H]$ = 1.0 for all the elements. However, the observed UV excess shortward 1650 Å , where the Si discontinuities occur, cannot be explained with Si underabundance, because abundance analyses by Adelman (1973) and Savanov & Malanushenko (1990) yielded about solar abundance for it. Our abundance analysis has given solar abundance as upper limit for Si (Table 4).

A more plausible possibility is that the companion is a λ Boo star about 1.5^m visual magnitude fainter than β CrB$_A$, metal poor ($[M/H] = -1.0$) and fast rotating, in order to explain the fact that no spectral lines of β CrB$_B$ are observable. From the mass function $f(M)$ = 0.24, i = 111° (Kamper et al., 1990), assuming a mass ratio R = 1.7, as suggested by the magnitude difference of about 1.6^m, we find a mass of 2.16 solar masses for β CrB$_A$, and of 1.27 for β CrB$_B$, with a total mass of the system of 3.43 M$_\odot$ in agreement with the value given by Kamper et al. of 4.3 M$_\odot$ $\pm$ 2.0 M$_\odot$.

From Table 4, we note that there is generally good agreement among the abundances derived by Hack (1958), Adelman (1973), Savanov & Malanushenko (1990), and the present work. Some relatively small discrepancies must be partly imputed to the variability of the equivalent widths of several elements and partly to different atmospheric models and different values of the $\log gf$ used in the determination of the abundances. One can synthesize the chemical peculiarities of β CrB as follows: a defect of light elements like C , N , Al , possibly Si , an excess by a factor of about 10 for the iron group, and excesses by factors ranging from 10^2 to 10^4 for heavy elements and Rare Earths.

A possible explanation for the behavior of the Li blend is the spotted distribution of lithium and other components of the blend. The lists of lines in the Li region given by Gerbaldi et al. (1995) and by Burkhart & Coupry (1991) suggest that the influence on lithium doublet of blending lines should be minor. However, in the case of β CrB the feature at λ 6708 Å cannot be explained by assuming an anomalous large Li^6/Li^7 ratio, but rather by assuming that Li is blended with some unidentified line, or possibly with the V I line at λ6708.094Å. However, in this last case, a very unlikely vanadium overabundance by a factor 10^3 has to be proved. Another source of uncertainty is the not sufficient precision in the wavelength scale. We have made correction to the wavelength scale after a critical analysis of the binary radial velocity curve. The accuracy of the value of the γ - velocity is of 1.4 - 2.5 km s^{-1}. New more precise determinations of the orbital parameters should be necessary.

The complex relations between the equivalent widths, the FWHM, and the radial rotational velocity V_r versus the rotational phase suggest that the various elements are concentrated in one or several spots. However much more observations are necessary, in order to cover completely the rotational period. Moreover a better knowledge of the law of variation of the equivalent widths of several elements is needed for a more accurate determination of the abundance peculiarities. However this is the first indication and observational evidence of "spotness" for a slowly rotator cold SrCrEu star with a large magnetic field.

Acknowledgements. We wish to thank the referee Dr. F. Spite for many useful suggestions. This research was supported in part by the National Group of Astronomy of the National Council of Research (CNR-GNA)

and by the Regional Interuniversity Center for Astrophysics and Cosmology (CIRAC)

References

Adelman, S.J. 1973, ApJ, 183, 95
Anders, E., Ebihara,M. 1982, Geochim. Cosmochim. Acta, 46, 2363
Anders, E., Grevesse, N. 1989, Geochim. Cosmochim. Acta, 53, 197
Breger, M 1976 ApJS, 32, 7
Burkhart, C., Coupry, M.F. 1991, A&A, 249, 205
Faraggiana R, Gerbaldi M., Castelli F., Floquet, M. 1986 A&A 158, 200
Faraggiana, R., Gerbaldi, M. 1992, Proceed. Coll. IAU, No 138, p.169
Faraggiana, R., Hack, M. 1963, PASP, 75, 376
Gerbaldi, M., Faraggiana, R. 1991, Mem. Soc. Astron. Ital., 62, 97
Gerbaldi, M., Faraggiana, R., Castelli, F. 1995, A&AS, 111, 1
Griffin, R.E.M., Griffin, R.F. 1979, A photometric Atlas of the Spectum of Procyon, Cambridge
Hack, M. 1958, Mem. Soc. Astron. Ital., 29, 263
Hatzes, A.P. 1991a, MNRAS, 248, 487
Hatzes, A.P. 1991b, MNRAS, 253, 89
Jamar, C., Macau-Hercot, D., Monfils, A., Thompson, G.I., Houziaux, L., Wilson, R. 1976, Ultraviolet Bright - Star Spectrophotometric Catalogue, ESA SR-27
Kamper, K.W., McAlister, H.A., Hartkopf, W.I. 1990, AJ, 100, 239
Kurtz, D.W., Martinez, P., Tripe, P. 1994a, MNRAS, 271, 421
Kurtz, D.W., Martinez, P., van Wyk, F., Marang, F., Roberts, G. 1994b, MNRAS, 268, 641
Kurtz, D.W., Sullivan, D.J., Martinez, P., Tripe, P. 1994c, MNRAS, 270, 674
Kurucz, R.L. 1993a, CD-ROM No 13
Kurucz, R.L. 1993b, CD-ROM No 18
Kurucz, R.L. 1995, ApJ, 452, 102
Lambert,D.L., Smith V.V., Heath, J. 1993, PASP 105, 568
Landstreet, J. 1996, Proceed. of the Vienna workshop on "Model Atmospheres and Spectrum Synthesis", July 1995, ASP Conference Series, eds. S. Adelman, F. Kupka and W.Weiss, in press.
Mathys, G. 1995, A&A, 293, 746
Nave, G., Johansson, S., Learner, R.C.M., Thorne, A.P., Brault, J.W. 1994, ApJS, 94, 221
Neubauer, F.J. 1944, ApJ, 99, 134
Oetken L., Orwert R., 1984, Astron. Nachr., 305, 317
Polosukhina, N. S., Lyubimkov, L. S. 1995, Mem. Soc. Astron. Ital., 66, 361
Polosukhina N.S., Malanushenko V.P. 1995, poster presented at the Joint European and National Astronomy Meeting, JENAM-95, Catania, Italy, Sept 25-29, in press
Preston, G.W., 1967, ApJ, 150, 547
Pyper, D.M., Adelman, S.J. 1985, A&AS, 59, 369
Savanov, I.S., Malanushenko, V.P. 1990 Afz, 33, 243
Sergeev, S. 1996, Program SPE , in press
Smith V.V., Lambert D.L., Nissen P.E. 1993, ApJ 408, 262

This article was processed by the author using Springer-Verlag LaTeX A&A style file *L-AA* version 3.